LIMNOLOGY
and
OCEANOGRAPHY

ASLO

Limnol. Oceanogr. 9999, 2022, 1–16

doi: 10.1002/lno.12008

Deep-sea wooden shipwrecks influence sediment microbiome diversity

Justyna J. Hampel,[1] **Rachel D. Moseley**,[1] **Rachel L. Mugge**,[1] **Anirban Ray**,[1] **Melanie Damour**,[2] **Douglas Jones**,[2] **Leila J. Hamdan**[1]*

[1]Division of Coastal Sciences, School of Ocean Science and Engineering, University of Southern Mississippi, Ocean Springs, Mississippi

[2]Bureau of Ocean Energy Management, New Orleans, Louisiana

Abstract

Historic shipwrecks function as habitats for benthic organisms by providing food, refuge, and structure. They also form islands of biodiversity on the seabed, shaping microbial ecology and ecosystem processes. This study examined two wooden deep-sea shipwrecks at 525 and 1800 m water depth and probed their influence on sediment microbiomes and geochemistry. Microbiomes were investigated with 16S rRNA gene amplicon sequencing along 60 m transects extending in four directions from the hulls of the shipwrecks. Distance from shipwrecks and sediment depth both shaped microbiome structure. Archaeal alpha diversity was significantly and positively correlated with proximity to the deeper shipwreck while bacterial diversity was not to either. Archaeal community structure differed at both sites; the deeper site had a higher proportion of Bathyarchaeia and Lokiarchaeia proximate to shipwreck compared to the shallow location. Major bacterial communities were consistent at both sites, however, at the deeper site had higher abundance of Bacteroidetes, Chloroflexi, Desulfofarculales, and Desulfobacteriales. Core microbiome and differential abundance analyses revealed unique taxa nearest the shipwrecks compared to the surrounding seabed including organoheterotrophs, and cellulolytic and sulfur cycling taxa. Sediment carbon content influenced microbiome structure near the shipwrecks (5–10 m). We show that shipwrecks have a distinct sediment microbiome and form unique habitat patches on seabed, resembling those surrounding organic falls. The shipwreck influence was more pronounced at the deeper site, further from terrestrial influences signaling shipwrecks may be a significant source of organic matter in far-shore oligotrophic settings.

Deep-sea sediments (below 200 m) account for majority of Earth's surface, forming one of the largest ecosystems on the planet (D'Hondt et al. 2004; Orcutt et al. 2011). In the absence of light, where extreme temperatures, steep redox gradients, and high pressure exist, unique habitats for benthic microfauna and macrofauna form. Marine sediments are diverse with regionally and globally distinct populations (Zinger et al. 2011; Ruff et al. 2015; Thompson et al. 2017). Microbial cell abundance in marine sediment is up to 10,000-fold greater per unit volume than the ocean surface (Jørgensen and Boetius 2007), and the majority of deep-sea microbes have not been cultured despite their importance to marine carbon and nutrient cycling.

Bacteria, archaea, and viruses in marine sediments control a large portion of carbon storage and are an important link in global biogeochemical cycles (Breitbart 2012; Orsi 2018). In the deep sea, microbial life relies on the biological carbon pump, sinking organic matter (OM) from the euphotic zone, or chemolithotrophy (Zinger et al. 2011; Bienhold et al. 2013). Natural (reefs, hydrothermal vents, cold seeps) and artificial features on the seabed alter the local environment, biogeochemistry, microbial community composition and diversity (Zinger et al. 2011; Bienhold et al. 2013; Hamdan et al. 2021). To date, the majority of microbial ecology studies in marine sediments have focused on geological features such as hydrothermal vents and hydrocarbon seeps, which are considered hotspots of biological activity and diversity (Orcutt et al. 2011; Anderson et al. 2015; Ruff et al. 2015) and select for phylogenetically distinct microbial communities (Dick 2019) and metabolic pathways (Dombrowski et al. 2018).

Organic falls (wood and organismal) are natural seafloor features that attract benthic organisms and result in focused locations of high biodiversity. Whale and wood fall studies display high microbial diversity in nearby sediments, forming biological hotspots (Fagervold et al. 2012; Bienhold et al. 2013; Smith et al. 2015) and spheres of influence (increased species diversity and richness; Smith et al. 2015). Organic falls often harbor distinct microbial communities relative to the surrounding seafloor associated with highly

*Correspondence: leila.hamdan@usm.edu

Additional Supporting Information may be found in the online version of this article.

reduced, chemosynthetic environments (Fagervold et al. 2012; Bienhold et al. 2013; Smith et al. 2015). High OM content from organic falls shapes seafloor microbiomes and function (Bienhold et al. 2013) leading to increased remineralization and establishment of steep redox gradients relative to the surrounding sediment (Kalenitchenko et al. 2016). Such conditions favor chemotrophic processes and presence of sulfide-oxidizing and sulfate-reducing bacteria, fermenters, and anaerobic cellulolytic bacteria (Goffredi and Orphan 2010; Ristova et al. 2017). Over time, organic fall environments resemble hydrothermal vents with distinct and diverse microbial communities, biogeochemical processes, and can serve as an important nutrient source in the oligotrophic ocean (Fagervold et al. 2012; Bienhold et al. 2013; Kalenitchenko et al. 2016) whereas over shorter durations compared to geological features.

Although many microbiome studies have focused on natural features on the seabed, built environments (e.g., artificial reefs, shipwrecks, oil, and gas infrastructures) are frequently overlooked. Historic shipwrecks (> 50 years old) can be viewed as islands of microbial biodiversity, similar to natural seafloor features (Hamdan et al. 2018, 2021). They provide food, refuge from predation, hard substrate for microbial colonization, and assist in dispersal and recruitment of microorganisms and macrofauna (Walker et al. 2007; Hamdan et al. 2018; Mugge et al. 2019). Moreover, some built environments are composed of materials not naturally occurring on the seabed (metal, plastic, composites; Mugge et al. 2019). Large, metal-hulled shipwreck isolated on seabed influenced sediment microbiome diversity and richness, resulting in an increase in both with proximity and extending outward 200 m onto the seabed (Hamdan et al. 2021). The size and composition of these halos of biodiversity are dictated by the time since shipwreck arrival on seabed, since their increase in size may be in response to hull degradation and resource utilization (Stieglitz 2013; Reeds et al. 2018), along with physical alterations of sediment resulting from the presence of a high relief (> 1 m) structure (Harris 2014).

Wooden-hulled shipwrecks may provide OM similar to natural falls (Bienhold et al. 2013), with potential to shape sediment biogeochemistry in similar ways, but are more complex (e.g., mixed materials), have variable size and relief, and accordingly, the magnitude of their effect on the surrounding seabed may vary both spatially and temporally relative to natural features (Hamdan et al. 2018). The northern Gulf of Mexico provides opportunities to study built environments on the seafloor with more than 2000 reported historic shipwrecks spanning 500 years of history (Damour et al. 2015). Although the Gulf of Mexico has been a subject of many sediment microbiome studies (Mason et al. 2014; Overholt et al. 2019; Zhao et al. 2020a), an information gap arises regarding built structures and their regional impacts on microbial ecology (Hamdan et al. 2018). Considering the numerous shipwrecks, and approximately 6000 oil and gas-related structures on the seafloor, it is important to investigate impacts of built structures on microbial life in deep-sea sediments.

Here, we aimed to (1) characterize the sediment microbiome surrounding two historic wooden-hulled deep-water shipwrecks at different water depths in the northern Gulf of Mexico (Fig. 1), (2) examine changes in microbiome composition and core members of microbiomes with proximity to the shipwrecks to identify shipwreck-associated taxa, and (3) determine how wooden-hulled shipwrecks influence biogeochemistry in deep-sea sediments. We hypothesized microbiome composition in the local environment changes as a function of distance from a shipwreck (up to 60 m away) and that microbial diversity will be greatest near shipwrecks and will decrease outward. We also hypothesized that sediments near wooden shipwrecks will have a unique core microbiome, relative to microbiomes in reference sediments from the surrounding seabed. Finally, we posit that the presence of a shipwreck changes the carbon and nitrogen biogeochemistry of the surrounding seabed.

Materials

Site description and sample collection

The two shipwrecks selected for this study are located in the northern Gulf of Mexico (Fig. 1) and were investigated for the first time during this work. Both were detected by sonar during geophysical surveys in 2009 and 2013. Site 15711 (hereafter referred as the "shallow") is a wooden-hulled, copper-sheathed sailing vessel likely dating between the last quarter of the 19th century and the first decade of the 20th century. It is located at ~ 525 m water depth in the Viosca Knoll lease area and measures 20 m long by 7 m wide. The shipwreck at the shallow site is oriented with the bow facing west-southwest. It exhibits approximately 1.5–3 m of vertical relief and debris fields extending from a few to several meters out from the hull in some areas. The second shipwreck, site 15470 (hereafter referred as the "deep" site), is a wooden-hulled, copper-sheathed sailing vessel, also likely dating to the late 19th century and located at ~ 1800 m water depth in the Mississippi Canyon lease area. The site measures 32 m long by 12.5 m wide with approximately 0.8–1.3 m vertical relief. The observed debris field was limited to within a few meters of the hull and consisted of collapsed vessel elements. The shipwreck at the deep site is oriented with the bow pointing west-southwest at ~ 255°.

Sample collection took place in June and July 2019, during the PS19-24 expedition on board Research Vessel *Point Sur* (University of Southern Mississippi). Sediment samples were collected with Jason-style push cores (20 cm in length) by remotely operated vehicle *Odysseus* (Pelagic Services). Before sampling, archeological surveys were completed to identify suitable sampling areas free of archeological debris. Sediment samples were collected along four lateral transects at 4–7 m (hereafter refer to as 5-m group), 10 m, 18–20 m (hereafter refer to as 20-m group), 40 m, and 57–60 m (hereafter refer to as 60-m group) distance intervals from each shipwreck hull.

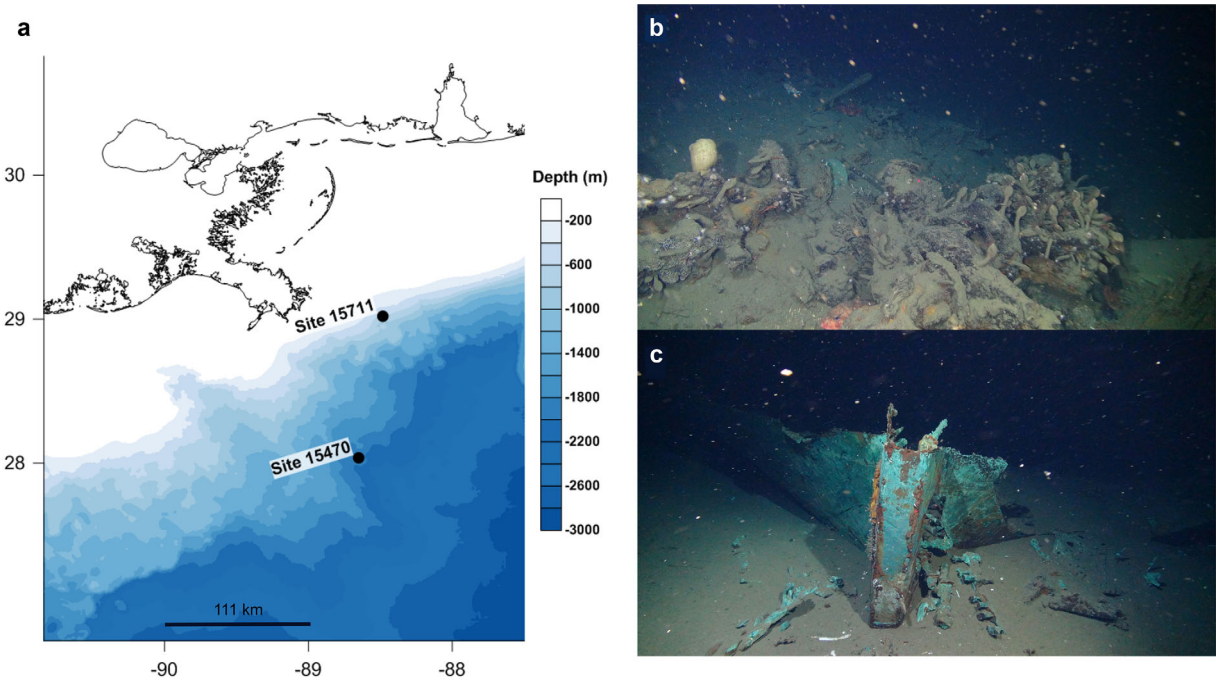

Fig 1. Sampling locations in the northern Gulf of Mexico. Sites 15711 and 15470 are referred to in the text and hereafter as "shallow" and "deep," respectively (**a**). Remotely operated vehicle image of the sites 15711 (**b**) and 15470 (**c**).

Transects extended from the bow, stern, and along two perpendicular axes from the port and starboard midships area. Distance was confirmed using the onboard sonar and an ultrashort baseline beacon on the remotely operated vehicle. Sediment cores were extruded shipboard as described in Hamdan et al. (2018) and sampled at 4 cm depth resolution down to 16 cm below the seafloor (cmbsf) into 15-mL Polymerase chain reaction (PCR) clean polycarbonate conical tubes (Falcon) for DNA analysis, and into 4-oz Whirl-Pak® storage bags for sediment geochemistry analyses. Samples for porosity were collected in 100 mm × 15 mm snap cap petri dishes (Fisherbrand™). Replicate cores were collected at the 5, 20, and 60 m distances on all transects to facilitate pore-water nutrient analysis. Up to 30 mL of pore-water was extracted at 4, 8, and 12 cmbsf using the 0.1-μm Rhizon samplers (Rhizosphere Research Products) and decanted into separate 2-mL glass vials for subsequent analyses (Hamdan et al. 2013). Samples for molecular analysis were immediately frozen and stored at −80°C until DNA extractions. Pore-water samples were frozen at −20°C and porosity samples were stored at 4°C.

DNA extraction and sequencing

Genomic DNA from sediment was extracted with FastDNA® SPIN kit (MP Biomedical) as previously described (Hamdan et al. 2018). Extracted DNA was quantified on a Qubit 2.0 Fluorometric Quantitation system (Invitrogen) and checked for purity with NanoDrop spectrophotometer (ThermoFisher). Genomic template DNA was sent to Integrated Microbiome Resource facility (Dalhousie University) for 16S rRNA gene amplification, library preparation, paired-end 2 × 300 bp Ilumina MiSeq sequencing, and demultiplexing following the established protocols (Comeau et al. 2011; Salerno et al. 2018). The bacterial and archaeal 16SrRNA V6-V8 variable regions were targeted for amplification using B969F/BA1406 and A956F/A1401R primer sets, respectively (Comeau et al. 2011).

Bioinformatics analysis

Bioinformatics analysis of raw archaeal and bacterial amplicon sequences was conducted using the Quantitative Insights into Microbial Ecology 2 (QIIME2) platform (Bolyen et al. 2019). Sequences were trimmed and quality controlled using DADA2 (Callahan et al. 2017) for paired-end sequences at default settings. The resulting amplicon sequence variant feature table (output from DADA2) was clustered de novo into operational taxonomic units (OTUs) based on 97% identity using VSEARCH. Amplicon sequence variants were clustered into OTUs to avoid inflation of alpha diversity, as suggested in some studies (Glassman and Martiny 2018), while also implementing high-quality control by generating sequence variants through DADA2. Core metric diversity analyses (alpha and beta diversities) were conducted using the core-metrics plugin. Taxonomic assignment was made using the trained classifier (q2-feature-classifier) with extracted reads from the SILVA 132 reference database and VSEARCH classification. The core microbiome at each shipwreck and each distance group was determined with the feature-table

core-features plugin in QIIME2 using 85% as the minimum fraction of samples that a feature must be observed in. The 85% cutoff provides a balance between stringency of core members and specificity to distance groups. Community composition and alpha diversity plots were constructed in RStudio with PhyloSeq (McMurdie and Holmes 2013) and ggplot2 packages. Low abundance taxa (< 5%) were filtered for visualization purposes before constructing relative abundance plots. Raw sequences have been deposited to NCBI's Sequence Read Archive and are available under BioProject number PRJNA599410.

Sediment geochemistry and pore-water analysis

Porosity was determined gravimetrically, samples were dried at 60°C for 24 h, and porosity was determined from difference in wet and dry mass (Hamdan et al. 2018). A Delta V Advantage Isotope Ratio Mass Spectrometer (ThermoFisher) coupled with an elemental combustion system (Costech ECS 4010) were used to determine sediment total carbon (TC) and total nitrogen (TN), and stable carbon ($\delta^{13}C$) and nitrogen ($\delta^{15}N$) isotope ratios along one transect at each site. About 3 mg of dried, ground sediment was weighed using a microbalance and packed into pressed tin capsules (5 × 9 mm, Costech Analytical Technologies). Acetanilide was used to create a calibration curve for the analysis. Ammonium pore-water concentration was determined spectrophotometrically following the salicylate–hypochloride method (Bower 1980). Pore-water nitrate and nitrite concentration (NO_x) was determined using chemiluminescence analyzer (Thermo) following the vanadium reduction to NO method (Braman and Hendrix 1989). Sulfate concentration was determined by ion chromatography (Methrom, IC Compact 761) at the University of California Los Angeles (Treude et al. 2020).

Statistical analysis

PRIMER (v. 7) with PERMANOVA+ was used for statistical analysis of microbiome composition (Clarke and Gorley 2015). Bray–Curtis dissimilarities were calculated from the archaeal and bacterial OTU abundance tables. Nonmetric multidimensional scaling ordination plots were constructed to visualize similarities in microbiome structures. Hierarchical clustering based on the group average linkage was used to generate dendrograms to explain similarity among groups of samples. A permutational multiple ANOVA (PERMANOVA) identified differences in the community composition based on the variables site, distance, and sediment depth. PERMANOVA was run using Type III (sequential) sum of squares, fixed effects sum to zero, permutation of residuals under a reduced model, and 9999 permutations. Diversity indices and geochemical data were checked for normality using Shapiro–Wilk test in RStudio. Subsequently, on determining data were nonparametric, Kruskall–Wallis test was used to find differences between sites and distance groups. Relationships between microbiome composition and geochemical variables were evaluated with Phyloseq and Vegan packages using the Constrained Analysis of Principal Coordinates (CAP) ordinations of Bray–Curtis dissimilarity tables after removing missing values from environmental data. Differentially abundant taxa were determined with beta binomial regression models using the "corncob" R package (Martin et al. 2020).

Results

Microbial diversity

From 160 sediment samples, over 11 million raw sequences were generated. Quality filtered archaeal features clustered into 1295 OTUs while bacterial features formed 13,759 OTUs at 97% similarity. Alpha diversity was higher in bacteria than in archaea at both sites (Fig. 2; Supporting Information Fig. S1). Archaeal Shannon diversity and OTU richness were higher at the shallow site than at the deep site (Fig. 2a; Kruskal–Wallis; $p < 0.001$). In contrast, bacterial diversity and richness were higher at the deep site (Fig. 2b; Kruskal–Wallis; $p < 0.001$). Diversity and richness of the archaeal community at the deep site significantly decreased with distance from the hull of the shipwreck (Fig. 2a; Kruskal–Wallis; $p < 0.01$). Archaeal diversity was lowest in surface sediments (0–4 cm) and increased with sediment depth (Supporting Information Fig. S1a). In contrast, bacterial diversity decreased with sediment depth (Supporting Information Fig. S1b).

Nonmetric multidimensional scaling of the Bray–Curtis dissimilarity revealed archaeal communities formed distinct clusters separated by study site and sediment depth (Fig. 3; Supporting Information Fig. S2). Some separation was also evident based on distance from the shipwrecks. At the deep site, archaeal samples in near proximity to the shipwreck formed a distinct cluster. Bacterial communities also clustered primarily by site. Samples from the deep site formed two large groups organized by distance from the shipwreck. The shallow site samples were more loosely organized (Fig. 3). Microbial communities did not differ between sampling transects (PERMANOVA; $p = 0.8$); therefore, subsequent analyses used averaged transect data.

Microbiome composition

Thaumarchaeota was the most abundant archaeal phylum at the shallow site (mean = 46% ± 5%) followed by Crenarchaeota (mean = 31% ± 4.2%) and Asgardaeota (mean = 14% ± 1.8%; Fig. 4a). The most abundant classes were Nitrososphaeria, Bathyarchaeia, and Lokiarchaeia, respectively. At the deep site, abundance of Thaumarchaeota was higher than at shallow site (mean = 83% ± 15%), followed by Euryarchaeota (mean = 5% ± 2.2%) and Crenarchaeota (mean = 5% ± 7.2%). Thaumarchaetoa density increased with distance from deep site while Asgardaeota, Crenarchaeota, Euryarchaeota, and Hydrothermarchaeota abundance decreased (Fig. 4a). At the deep site, there were pronounced

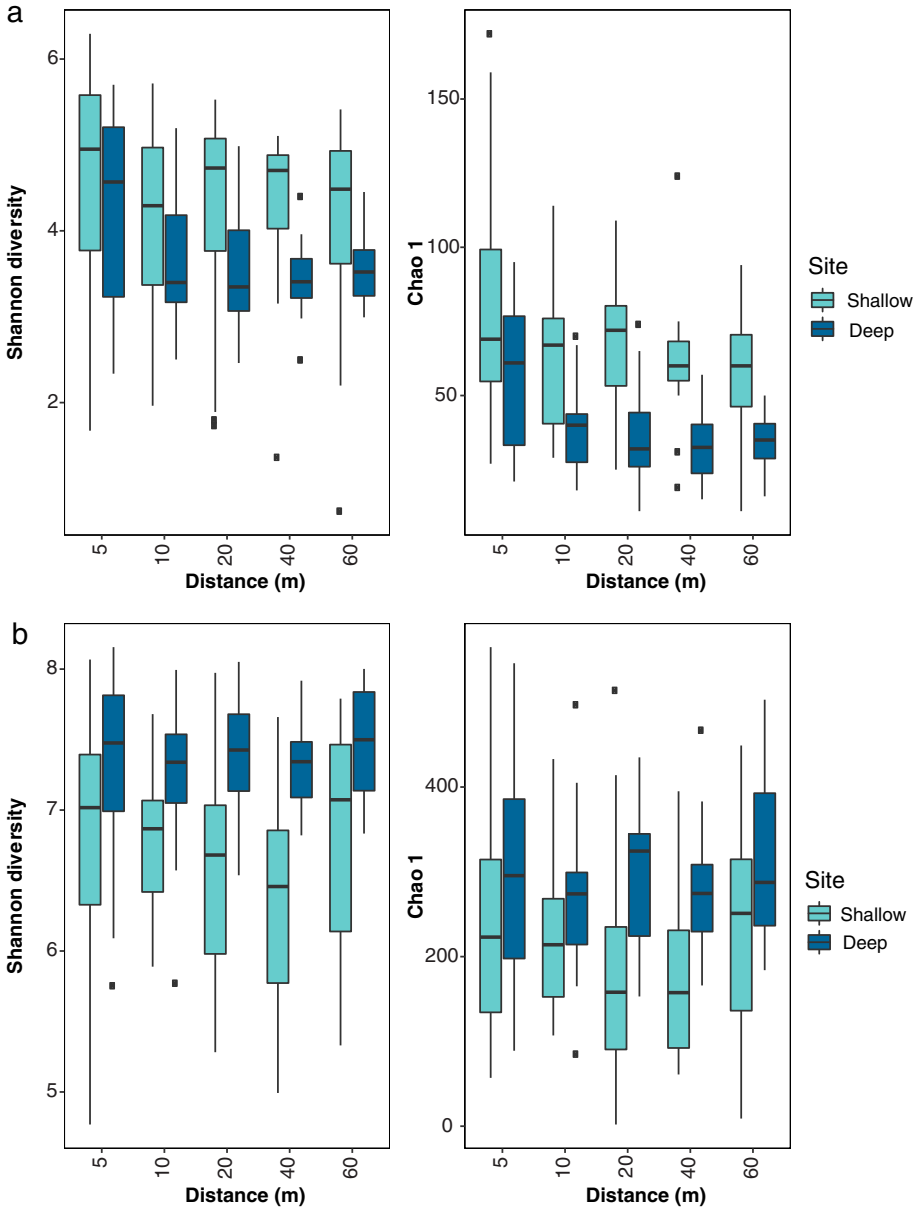

Fig 2. Alpha diversity plots with distance from shipwrecks for archaea (**a**) and bacteria (**b**) at two study sites.

differences in community structure concomitant with sediment depth where the abundance of Bathyarchaeia, Lokiarchaeia, Euryarchaeota; Thermoplasmata, and Nanoarchaeota; Woesarchaeia increased. Site, distance, and sediment depth were significant factors influencing archaeal community composition; the distance effect was more pronounced at deep site ($p = 0.001$) than at the shallow site ($p = 0.01$; Table 1).

Bacterial community at the shallow site was dominated by Proteobacteria (mean = 59% ± 3.8%), followed by Bacteroidetes (mean = 12% ± 1.9%) and Chloroflexi (mean = 3% ± 0.7%; Fig. 4b). Within the Proteobacteria phylum, Deltaproteobacteria were the most abundant class (mean = 49% ± 3%) followed by Gammaproteobacteria (mean = 29% ± 3.4%) and Alphaproteobacteria (mean = 22% ± 3%). Other abundant classes were Bacteroidia, Anaerolinea, and Dehalococcoidia. At the deep site, bacterial community composition had similar features with highest abundance of Proteobacteria (mean = 49% ± 4.4%) followed by Bacteroidetes (mean = 9% ± 2.3%), Chloroflexi (mean = 8% ± 1.5%), and Planctomycetes (mean = 7% ± 0.9%). Within the Proteobacteria, Deltaproteobacteria were most abundant class (mean = 41% ± 4.8%), followed by Gammaproteobacteria (mean = 30% ± 3%) and Alphaproteobacteria (mean = 29% ± 3.7%). At both sites, Bacteroidetes, Chloroflexi, and Deltaproteobacteria abundance decreased with distance from the shipwrecks. Site, distance from

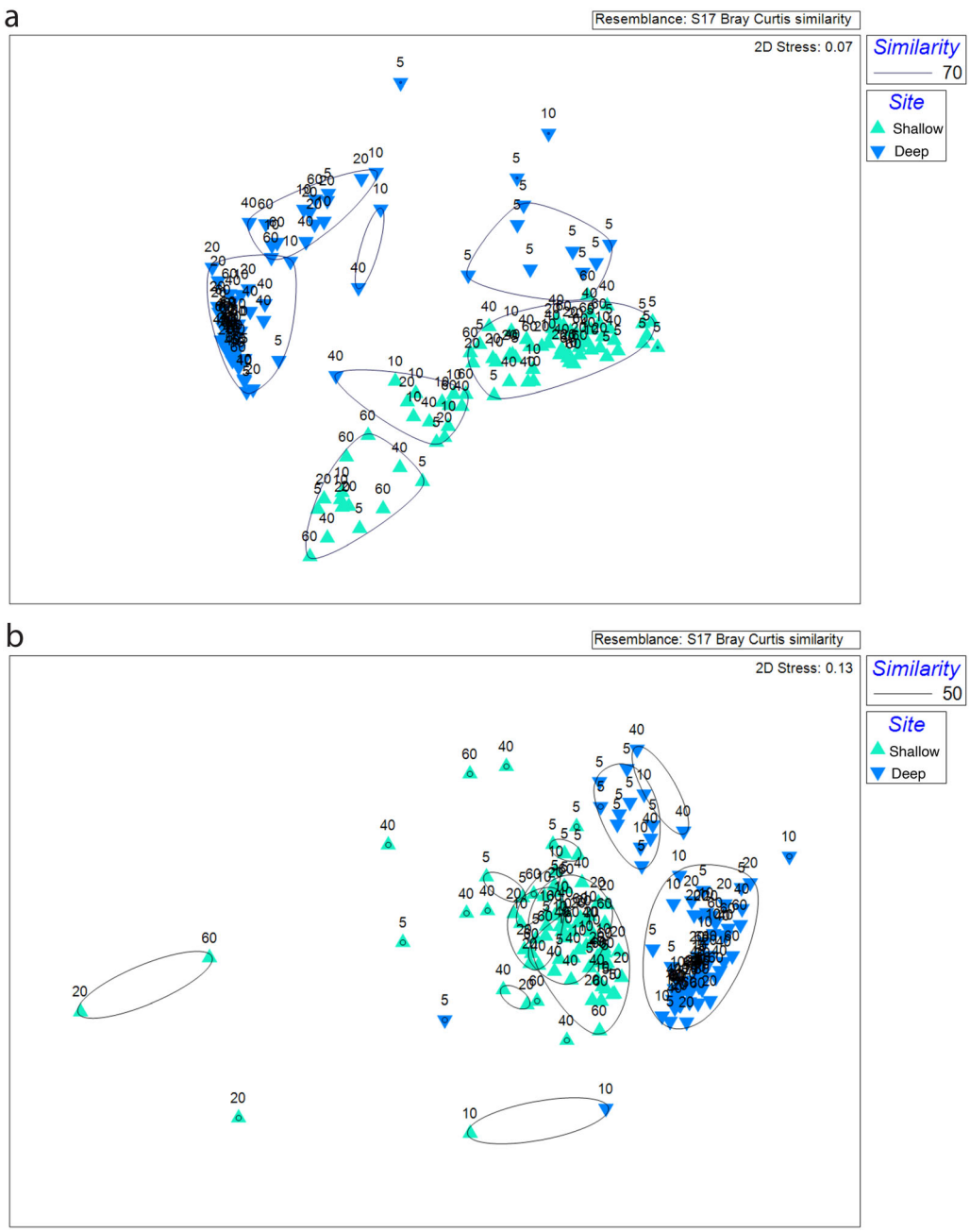

Fig 3. Nonmetric multidimensional scaling analysis of archaeal (**a**) and bacterial (**b**) communities at two shipwreck sites. Hierarchical clustering was used to obtain similarity dendrograms, based on the group average linkage, which are projected on the plot as contours. The numbers on the plots correspond to proximity to the shipwreck (m).

shipwreck, and sediment depth all significantly influenced bacterial composition ($p < 0.001$; Table 1).

Core microbiome

Membership in the core microbiome at each site and each distance was determined based on detection in 85% of the samples. The archaeal core microbiome at the shallow site was dominated by Crenarchaeota and Thaumarchaeota, and was uniform across distance from shipwreck. Most abundant core archaeal OTUs belonged to uncultured Bathyarchaeia and Lokiarchaeia and Ca. *Nitrosopumilus maritimus* (Fig. 5). The most abundant bacterial core OTUs were uncultured members of the Deltaproteobacteria NB1-j order, uncultured Bacteroidetes BD2-2, and uncultured Gammaproteobacteria (Fig. 6). The bacterial core microbiome nearest the shallow site (5 m) also consisted of less abundant taxa not present at further distances including uncultured Zixibacteria, Kiritimatiellaeota, Ignavibacteriales, and Desulfobulbaceae.

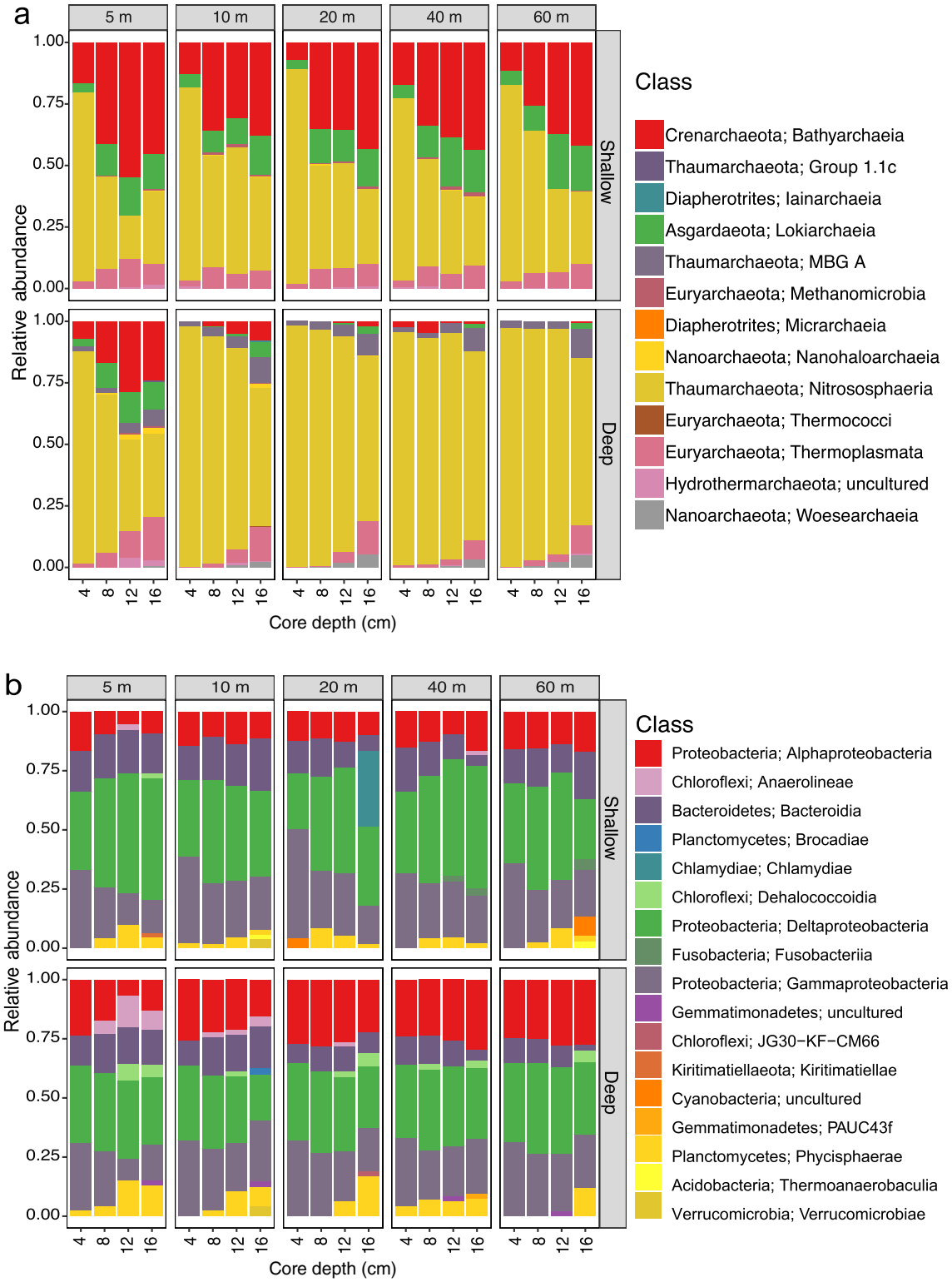

Fig 4. Relative abundance of class level community composition for archaea (**a**) and bacteria (**b**) with distance (facets) and core depth (*X*-axis). Low abundance taxa (< 5%) were filtered out prior constructing the plots.

The archaeal core microbiome at the deep site was almost entirely dominated by Thaumarchaeota (Fig. 5). The most abundant bacterial core OTUs at this site were uncultured members of Deltaproteobacteria NB1-j order, uncultured Cyclobacteriaceae, and Woeseia (Fig. 6). The near-shipwreck core microbiome included Ignavibacteriales, Anaerolineales,

Table 1. PERMANOVA conducted on sediment samples to determine differences in microbiome community similarity based on site locations and distance and depth in centimeter below seafloor from shipwrecks. PERMANOVA was run using Type III (partial) sum of squares, fixed effects summed to zero with permutation of residuals under a reduced model and 999 permutations.

Sites		Source	Degrees of freedom	Sum of squares	Mean sum of squares	Pseudo-*F*	*p* value	Unique permutations
Both	Archaea	Site	1	9.0E+04	89,870	109.5	**0.0001**	9938
		Residuals	158	1.3E+05	820.5			
		Total	159	2.2E+05				
	Bacteria	Site	1	5.9E+04	58,973	38.5	**0.0001**	9902
		Residuals	158	2.4E+05	1530.2			
		Total	159	3.0E+05				
Shallow	Archaea	Distance (m)	4	3.2E+03	811.7	2.24	**0.01**	9917
		Depth (cmbsf)	3	3.2E+04	10,781	29.8	**0.0001**	9951
		Distance × depth	12	4.1E+03	344.9	0.95	0.54	9883
		Residuals	60	2.2E+04	362.4			
		Total	79	6.1E+04				
	Bacteria	Distance (m)	4	8.8E+03	2199	1.48	**0.008**	9822
		Depth (cmbsf)	3	1.7E+04	5660	3.82	**0.0001**	9839
		Distance × depth	12	1.5E+04	1251	0.84	0.97	9641
		Residuals	60	8.9E+04	1482			
		Total	79	1.3E+05				
Deep	Archaea	Distance (m)	4	1.9E+04	4729	10.6	**0.0001**	9936
		Depth (cmbsf)	3	1.6E+04	5431	12.2	**0.0001**	9943
		Distance × depth	12	6.3E+03	521.6	1.17	0.25	9880
		Residuals	60	2.7E+04	444.9			
		Total	79	6.8E+04				
	Bacteria	Distance (m)	4	1.7E+04	4135	3.76	**0.0001**	9873
		Depth (cmbsf)	3	1.7E+04	5795	5.26	**0.0001**	9884
		Distance × depth	12	1.2E+04	1008	0.92	0.73	9779
		Residuals	60	6.6E+04	1101			
		Total	79	1.1E+05				

Numbers in bold denote statistical significance.

Dehalococcoidia, Syntrophobacterales, and Zixibacteria, present only at 5 m.

Differential abundance

Differential abundance analysis on archaeal and bacterial communities assisted with resolving shipwreck-taxa associations at both sites. Samples from the 5 m group were compared to the 60-m group, as the represented the end-members of the transect, and could provide information on differentially abundant OTUs based on proximity to sites. The analyses for the shallow site did not reveal statistically significant differentially abundant taxa for either archaea or bacteria, and thus no results are presented. At the deep site, differentially abundant archaea at 5 m (but not 60 m) belonged to uncultured Crenarchaeota, Euryarchaeota, Hydrothermarchaeota, Asgararchaeota, Hadesarchaeota, Diapherotrites, and Nanohaloarchaea phyla (Supporting Information Fig. S3). Differentially abundant bacteria at the deep site at 5 m were affiliated with Bacteroidetes, Chloroflexi, Firmicutes, Kirimatiellaeota, and Zixibacteria (Supporting Information Fig. S4).

Sediment geochemistry and porosity

Sediment TN, $\delta^{13}C$ and $\delta^{15}N$ isotope ratios, and C : N differed significantly between sites (Kruskal–Wallis, $p < 0.001$). At the shallow site, average TN and TC were 0.22% ± 0.02% and 3.58% ± 0.33%, respectively (Fig. 7); average C : N was 16.6. Sediment $\delta^{13}C$ of TC at the shallow site ranged from −8.73 to −11.4 and $\delta^{15}N$ ranged from 3.7 to 5.6. No variables at this site were significantly different between distance groups. At the deep site, TN was significantly lower than at the shallow site and averaged 0.1% ± 0.01%. TC content was 3.68% ± 0.44% and marginally decreased with distance ($p = 0.07$). The C : N averaged 35.9. Sediment $\delta^{13}C$ at the deep site was enriched compared to the shallow site and ranged from −0.76 to −7.29. Sediment $\delta^{15}N$ at the deep site increased significantly with distance from the site and ranged from 3.6 to 4.2 ($p = 0.01$). Sediment porosity was greater at the shallow site

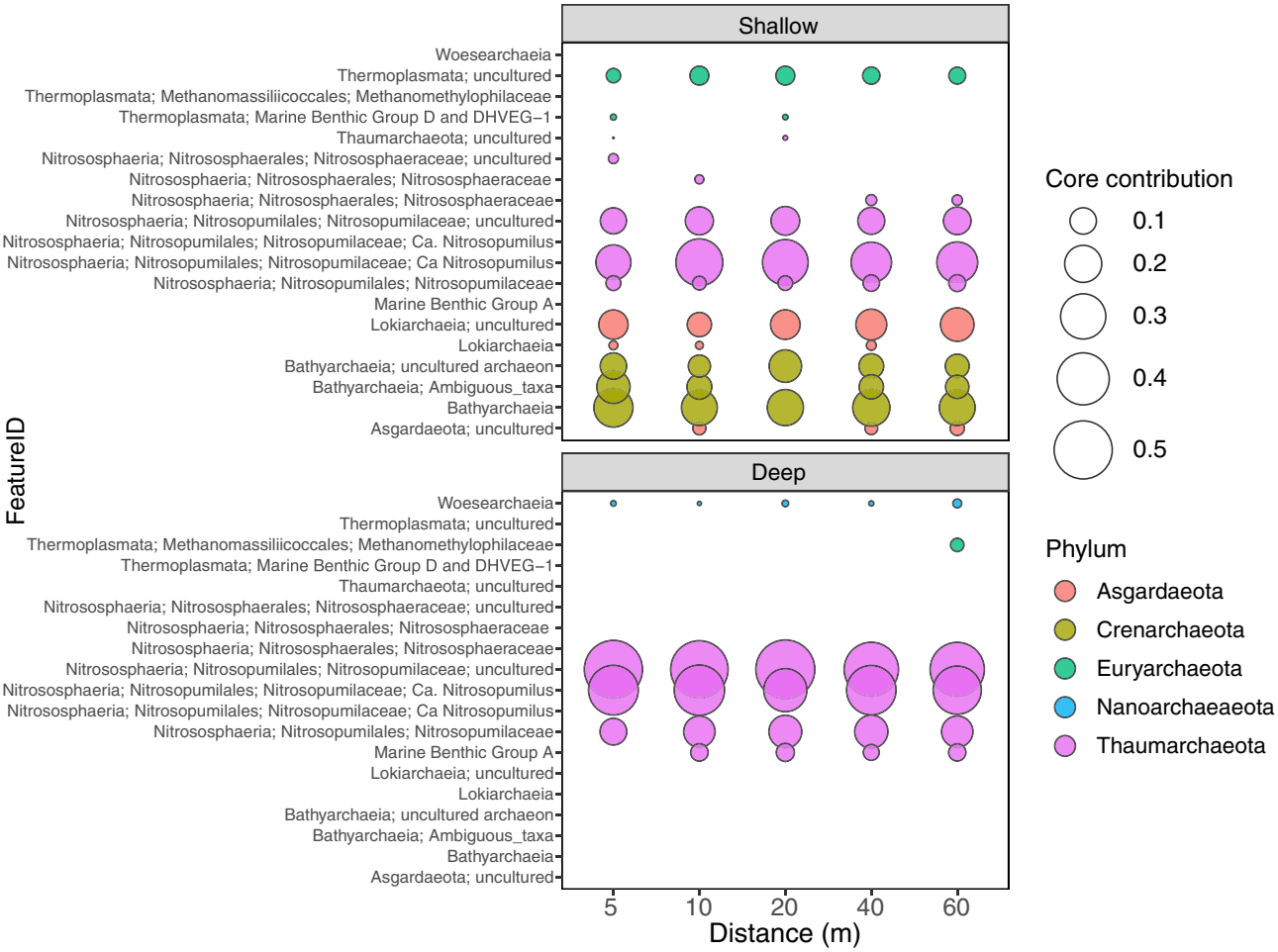

Fig 5. Archaeal core microbiome surrounding the shipwrecks present in 85% of the samples in each distance group. Core contribution (bubble size) represents the relative contribution of taxa to the core community in each distance group. Core members were identified to the lowest taxonomic level.

(84.8% ± 3.34%) than the deep (82.8% ± 2.12%; $p = 0.03$) and did not differ between distance groups at either site (Fig. 7). Porosity decreased with sediment depth at both sites.

Sediment cores for pore-water nutrient analysis were collected at 5, 20, and 60 m (Supporting Information Fig. S5). Ammonium concentration was significantly greater at the shallow site (52.3 ± 25.6 μM) than at the deep site (4.4 ± 2.91 μM; $p = 0.001$). In contrast, nitrate was greater at the deep site (17.2 ± 11.3 μM) than at the shallow location (0.55 ± 1.5 μM; $p = 0.02$) and decreased with depth. Average sulfate concentration did not differ between sites (28.1 ± 0.93 mM). Pore-water nutrient concentrations did not differ between distance groups.

To examine environmental influences on beta diversity, we performed a CAP on Bray–Curtis dissimilarity data. For archaea, the first two constrained axes together explained 41.5% of the total compositional variation (Fig. 8a). The most significant environmental variable in sediment correlating with the archaeal community structure along the CAP1 axis was TN ($r = 0.72$). Along CAP2 axis, porosity (0.91), and C : N ($r = -0.75$) were the most significant variables. For bacteria, CAP1 and CAP2 together explained 23.2% of community variation (Fig. 8b). The most significant environmental variables correlating with bacterial community structure were TN ($r = 0.91$) and C : N ($r = -0.81$) along the CAP1 axis, and porosity ($r = 0.84$) and TC ($r = -0.58$) along the CAP2 axis. Samples grouped by site, with TN driving community structure at the shallow site while C : N was an important variable at the deep site. Samples from 5 and 10 m at both sites grouped together and were driven by TC.

Discussion

Shipwreck sedimentary microbiomes and geochemistry

The goal of this study was to determine if and how the presence of wooden-hulled shipwrecks influence sediment microbiome composition and geochemistry. We compared two shipwreck sites separated horizontally by 111 km and vertically by ~1275 m of water. Natural features on the seabed are often spatially isolated and impact sediment microbiomes and

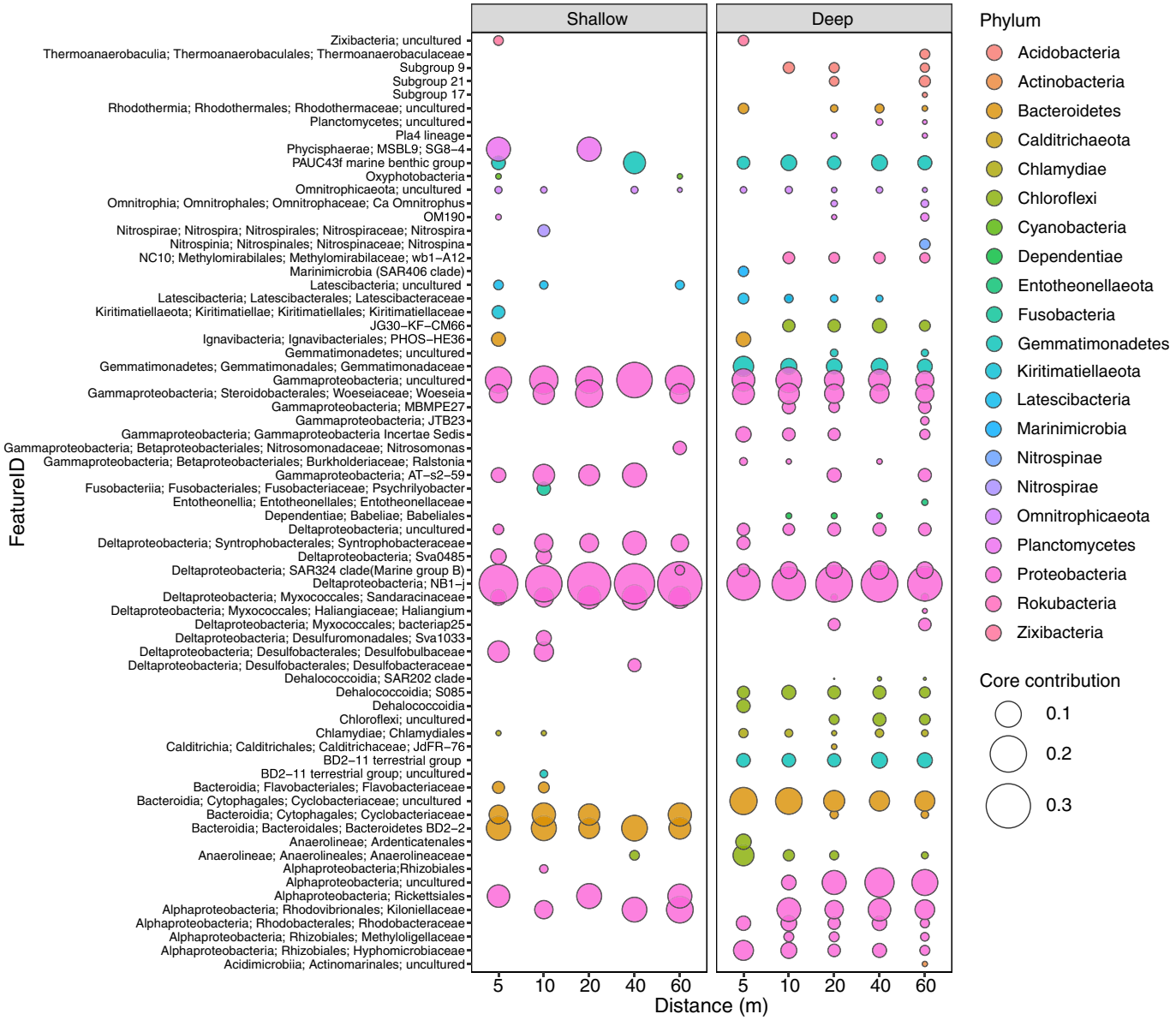

Fig 6. Bacterial core microbiome surrounding the shipwrecks present in 85% of the samples in each distance group. Core contribution (bubble size) represents the relative contribution of taxa to the core community in each distance group. Core members were identified to the lowest taxonomic level.

biogeochemistry. This study investigates if built environments have similar effects.

Alpha diversity of archaea was significantly influenced by proximity to the deep site but not the shallow one (Fig. 2a). In contrast, we observed no statistically significant distance effect on diversity of bacteria (Fig. 2b) at either site. These results are intriguing given that many organic fall studies (Goffredi and Orphan 2010; Fagervold et al. 2012) and previous shipwreck studies (Hamdan et al. 2018, 2021) report increased bacterial diversity with increasing proximity to features. Hamdan et al. (2021) reported increased bacterial diversity, and richness surrounding a larger steel-hulled historic shipwreck that extended up to 200 m on the seafloor. In that study, the relationship of proximity and diversity was nonlinear, and instead step-like at intermediate distances. This raises the possibility that a similar curvature is evident at sites in this study, but not fully captured as the transects terminate at 60 m distance from the hull.

Sediment microbiome structure differed between sites, with distance from shipwreck and with sediment depth at both locations (Table 1). It is not surprising to observe differences in community composition between sites given water depth and proximity to land (and Mississippi River discharge) are strong influencing factors on community composition (Kallmeyer et al. 2012; Mason et al. 2016; Hoshino et al. 2020). It is likely that sediments at the shallow site,

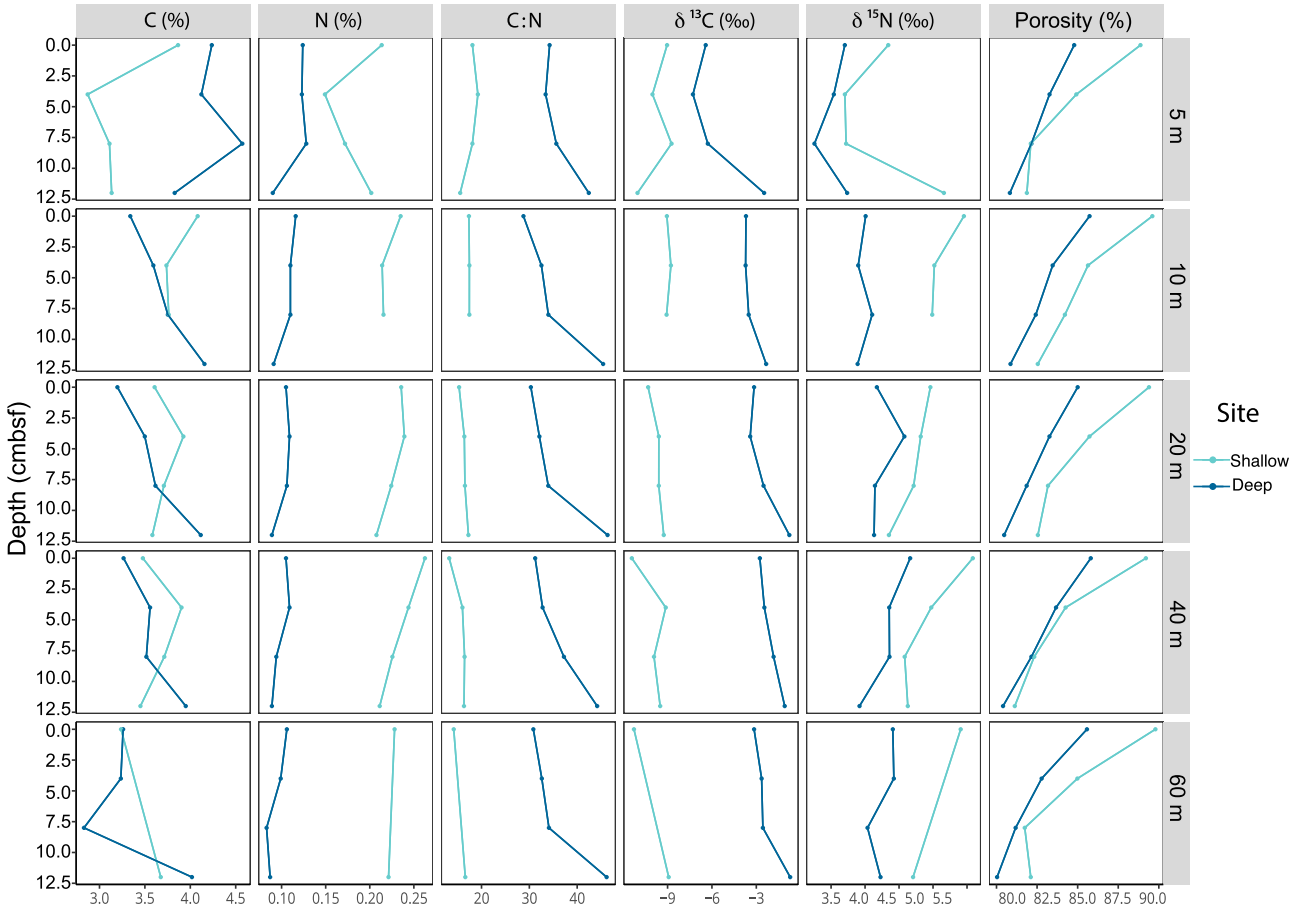

Fig 7. Depth profiles for sediment geochemistry with distance from shipwrecks.

76 km from the Mississippi River delta, receive more allochthonous carbon and nutrients and were more enriched in $\delta^{15}N$ than the deep site, which is consistent with isotopic signature of more productive sediments with riverine and coastal influence (Middelburg and Nieuwenhuize 1998). Sediments nearest to the hull of the deep site were more $\delta^{15}N$-depeleted, relative to further distance groups, and corresponded to values of terrestrial materials (Middelburg and Nieuwenhuize 1998). Easily degradable OM such as carbohydrates and amino acids are generally enriched in $\delta^{15}N$, in contrast to more recalcitrant compounds including lignin, a component of wood or other terrestrial OM (Ogrinc et al. 2005).

TC was not significantly different between sites, only marginally different with distance at the deep site, and $\delta^{13}C$ was more depleted near the shipwreck. Literature values of wood $\delta^{13}C$ vary between −25‰ and −28‰ and are more depleted than those of phytoplankton, diatoms, or plants (Fry and Sherr 1989). Overall, depleted $\delta^{13}C$ values at the shallow site might be indicative of high amounts of sinking phytoplankton and detritus while relatively depleted $\delta^{13}C$ near the deep site suggest the structure itself may be a source of OM. As organic carbon concentration was not measured, it is challenging to parse labile from refractory carbon.

Archaeal phyla in this study are consistent with other studies in surface (< 100 cmbsf) marine sediments (Lloyd et al. 2013; Overholt et al. 2019). We observed significant differences in the sediment community composition of archaea between the two sites (Fig. 3a) possibly due to the geographic separation of these locations from each other and the coast. Bathyarchaeia, highly abundant at the shallow site, are often found in organic-rich sediments of estuaries and coastal ecosystems, in anaerobic sediments (Hoshino et al. 2020) and are able to degrade a wide range of organic compounds including proteins, carbohydrates, and fatty acids (Zhou et al. 2018). Asgardeota are also abundant in anoxic marine and estuarine sediments, including the Gulf of Mexico (Hoshino et al. 2020) and use various organic substrates (Seitz et al. 2016). During sampling at the shallow site, we observed prolific sinking phytodetritus that could serve as a primary source of OM for microbial metabolism and explain higher abundance of anaerobic heterotrophic taxa at this site. While oxygen measurements were not made, pore-water sulfate was, and a drawdown in surface sediment sulfate observed at this site (Supporting Information Fig. S5) may indicate sulfate reduction fueled by OM degradation. High pore-water ammonium concentrations and depleted nitrate at the shallow site (Supporting Information Fig. S5) also

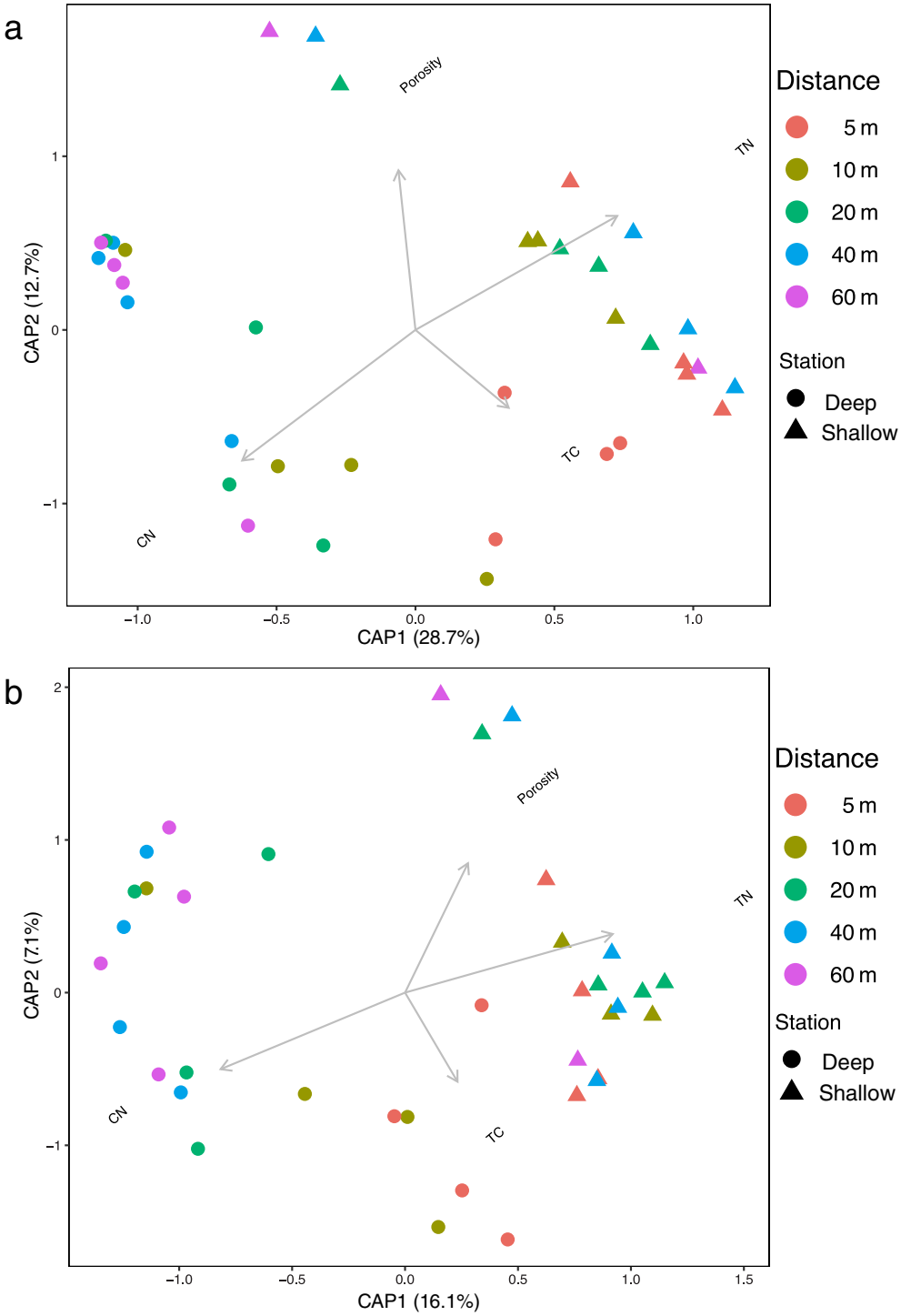

Fig 8. CAP plot of community dissimilarity (Bray–Curtis) between samples, color-coded by distance for archaea (**a**) and bacteria (**b**). Shapes correspond to the two sites, and vectors show significant environmental variables constraining the variability in community composition.

point to high remineralization rates. The high overall abundance of Thaumarchaeota at both locations is consistent with their ubiquity in the ocean (Stahl and De La Torre 2012; Tolar et al. 2020). Greater abundance of Thaumarchaeota at the deep site may be influenced by depth and relatively oligotrophic sediments vs. observations at the shallow site. At the deep site, Nitrosophaeria, class of ammonia-oxidizing archaea, accounted for 83% of the total archaeal community suggesting

chemolithotrophy is an important biogeochemical process and higher pore-water nitrate may be indicative of pronounced nitrification at the deep site.

Changes in archaeal microbiomes with distance were clearly pronounced at the deep site (Fig. 4a). Specifically, we observed increased abundance of Bathyarchaeia and Lokiarchaeia at 5 m relative to further distance groups. Bathyarchaeota can use various organic compounds including lignin and cellulose (Yu et al. 2018; Zou et al. 2020), which is the major component of wood and along with chitin represents important terrestrial carbohydrates in marine ecosystems (Bienhold et al. 2013; Ristova et al. 2017). Samples near the deep site (5 and 10 m; Fig. 8a) showed correlation between community structure and TC supporting a hypothesis that in oligotrophic areas removed from terrestrial sources of organic matter, a wooden shipwreck may be a significant energy source for shipwreck-associated archaea. However, gaps in knowledge exist regarding the specific metabolic pathways, archaeal genomes, and evolutionary adaptations in sediments surrounding these structures on the seafloor.

Bacterial community structure also differed between sampling sites (Fig. 3b) with TN and C : N as the main environmental drivers among parameters measured (Fig. 8b). Sediment communities at both sites were dominated by taxa ubiquitous in continental shelf sediments (Orsi 2018; Hoshino et al. 2020). Communities detected in this study were also in agreement with organic fall studies that report increased abundance of Desulfobulbacae, Desulfobacteracae, Bacteroidetes, and Firmicutes (Goffredi and Orphan 2010; Fagervold et al. 2012; Kalenitchenko et al. 2018) near these falls. Shipwreck degradation, like marine organic falls, may create niches for OM hydrolyzing bacteria such as Bacteroidetes, Cytophaga, and Flavobacteria which are known to break down complex organic compounds (Fagervold et al. 2012) and have been found in marine archeological wood samples (Landy et al. 2008).

As with archaeal microbiomes, we observed a distance effect at the deep site for bacteria with increased abundance of Bacteroidetes and Chloroflexi in 5-m sediments (Fig. 4b) relative to greater distances. The Chloroflexi class Anaerolinaea is general anaerobes and organoheterotrophs and include cellulolytic species (Podosokorskaya et al. 2013). Some members of the Chloroflexi phylum are known to consume recalcitrant carbon (Vuillemin et al. 2020) and degrade terrestrial OM (Colatriano et al. 2018), which may be relevant to wood degradation around shipwrecks. While community composition of Proteobacteria was consistent across distance at the shallow site (Supporting Information Fig. S6a), we observed increased abundance of Desulfofarculales and Desulfobacteriales near the shipwreck (Supporting Information Fig. S6b). Increased abundance of sulfur cycling taxa at 5 m from the hull of the deep site may indicate the presence of anoxic conditions and OM degradation. Sulfidic niches have also been associated with organic falls and waterlogged wood samples due to high rates of anaerobic mineralization of high OM content substrates (Fagervold et al. 2012; Bienhold et al. 2013; Kalenitchenko et al. 2015). This is supported by the strong correlation of bacteria in samples collected 5 and 10 m from the deep site with sediment TC (Fig. 8b). Overall, we show that although sediments surrounding wooden shipwrecks in the Gulf of Mexico have a consistent composition of bacteria with other Gulf of Mexico studies, unique taxa that may be specifically associated with the presence of a wooden structure on the seafloor are evident.

Shipwreck core microbiomes and differentially abundant taxa

Core microbiome analysis was performed to identify the persistent microbial consortia in each distance group and determine the presence of taxa occurring in association with shipwreck proximity. Core microbiome of archaea was vastly different between sites while core bacterial communities were consistent (Figs. 5 and 6). Taxa present solely in samples collected at 5 m included uncultured bacteria that are not highly abundant but may be functionally important to OM degradation at shipwrecks (Fig. 6, Supporting Information Fig. S3). Zixibacteria is a relatively newly discovered phylum and members have been found in marine sediments (Zinke et al. 2019), around hydrothermal vents (Dombrowski et al. 2017) and hydrocarbon seeps (Zhao et al. 2020b). Genome-centric studies of Zixibacteria identified pathways for complex OM breakdown (Zhao et al. 2020b), including cellulose and hemicellulose degradation (Baker et al. 2015; Dombrowski et al. 2017). Ignavibacteriales also contain cellulose and xylan degradation pathways and play a role in OM degradation (Woodcroft et al. 2018). These taxa, along with uncultured members of Bathyarchaeia, Asgardeota, Diphterotrites, and Hadesarchaeota, were identified as differentially abundant at the 5 m sampling site, relative to 60 m. It is likely these core microbiome members contribute to mineralization of more recalcitrant components of wood on the seafloor and fuel secondary decomposition by other microbes. Overall, we show that microbiomes in close proximity to wooden shipwrecks are distinct from the surrounding habitat, contain members potentially associated with wood degradation, and resemble other natural seabed features. The extent of influence of this shipwreck is comparable with that observed for organic falls (Smith et al. 2015). It is possible the shipwreck's influence on the surrounding seabed goes beyond the area examined in this study, based on observations of larger shipwrecks and their microbiomes (Hamdan et al. 2021). We note, however, the size and age of sites in the current study are smaller and older, respectively, than previously investigated locations. This may signal small wooden-hulled sailing vessels have a detectible, but less expansive imprint on the seabed than modern, steel-hulled wrecks with high relief.

Conclusions

In this study, we show that the extent of two historic wooden shipwreck's impact on seabed differs between sites and is likely due to difference in water column depth and proximity to OM supplied from riverine discharge. We posit that under oligotrophic conditions in the deep sea, shipwrecks are a relatively more important source of OM, become hotspots of microbiome diversity, and shape the surrounding seafloor microbiome with shipwreck-associated taxa. In the Gulf of Mexico, 53 shipwrecks have been visually confirmed to date in water depths below 1000 m (D. Jones, BOEM, pers. comm.). At least two dozen more uninvestigated sonar targets highly suggestive of deep-water shipwrecks have been discovered during recent geophysical surveys. Other areas in the Gulf of Mexico in water depths greater than 1000 m remain to be surveyed and may yield additional discoveries. These findings support the need for microbiological exploration of deep-water shipwrecks to learn how the arrival of human-made structures affects microbial composition and diversity of the deep seabed.

References

Anderson, R. E., M. L. Sogin, and J. A. Baross. 2015. Biogeography and ecology of the rare and abundant microbial lineages in deep-sea hydrothermal vents. FEMS Microbiol. Ecol. **91**: 1–11. doi:10.1093/femsec/fiu016

Baker, B. J., C. S. Lazar, A. P. Teske, and G. J. Dick. 2015. Genomic resolution of linkages in carbon, nitrogen, and sulfur cycling among widespread estuary sediment bacteria. Microbiome **3**: 1–12. doi:10.1186/s40168-015-0077-6

Bienhold, C., P. Pop Ristova, F. Wenzhöfer, T. Dittmar, and A. Boetius. 2013. How deep-sea wood falls sustain chemosynthetic life. PLoS One **8**: 10–15. doi:10.1371/journal.pone.0053590

Bolyen, E., and others. 2019. Reproducible, interactive, scalable and extensible microbiome data science using QIIME 2. Nat. Biotechnol. **37**: 852–857. doi:10.1038/s41587-019-0209-9

Bower, C. E. 1980. A simplified hydrazine-reduction method for determining high concentrations of nitrate in recirculated seawater. Aquaculture **21**: 281–286. doi:10.1016/0044-8486(80)90137-4

Braman, R. S., and S. A. Hendrix. 1989. Nanogram nitrite and nitrate determination in environmental and biological materials by vanadium(III) reduction with chemiluminescence detection. Anal. Chem. **61**: 2715–2718. doi:10.1021/ac00199a007

Breitbart, M. 2012. Marine viruses: Truth or dare. Ann. Rev. Mar. Sci. **4**: 425–448. doi:10.1146/annurev-marine-120709-142805

Callahan, B. J., P. J. McMurdie, and S. P. Holmes. 2017. Exact sequence variants should replace operational taxonomic units in marker-gene data analysis. ISME J. **11**: 2639–2643. doi:10.1038/ismej.2017.119

Clarke, K. R., and R. N. Gorley. 2015. Getting started with PRIMER v7. Plymouth, Plymouth Marine Laboratory, p. 20.

Colatriano, D., P. Q. Tran, C. Guéguen, W. J. Williams, C. Lovejoy, and D. A. Walsh. 2018. Genomic evidence for the degradation of terrestrial organic matter by pelagic Arctic Ocean Chloroflexi bacteria. Commun. Biol. **1**: 1–9. doi:10.1038/s42003-018-0086-7

Comeau, A. M., W. K. W. Li, J. É. Tremblay, E. C. Carmack, and C. Lovejoy. 2011. Arctic Ocean microbial community structure before and after the 2007 record sea ice minimum. PLoS One **6**: e27492. doi:10.1371/journal.pone.0027492

Damour, M., R. Church, D. Warren, C. Horrell, L. J., Hamdan. Gulf of Mexico Shipwreck Corrosion, Hydrocarbon Exposure, Microbiology, and Archaeology (GOM-SCHEMA) Project: Studying the Effects of a Major Oil Spill on Submerged Cultural Resources. 2016. Society for Historical Archaeology Annual Conference Proceedings, Seattle, WA: Society for Historical Archaeology.

D'Hondt, S., and others. 2004. Distributions of microbial activities in deep subseafloor sediments. Science **306**: 2216–2221.

Dick, G. J. 2019. The microbiomes of deep-sea hydrothermal vents: Distributed globally, shaped locally. Nat. Rev. Microbiol. **17**: 271–283. doi:10.1038/s41579-019-0160-2

Dombrowski, N., K. W. Seitz, A. P. Teske, and B. J. Baker. 2017. Genomic insights into potential interdependencies in microbial hydrocarbon and nutrient cycling in hydrothermal sediments. Microbiome **5**: 106. doi:10.1186/s40168-017-0322-2

Dombrowski, N., A. P. Teske, and B. J. Baker. 2018. Expansive microbial metabolic versatility and biodiversity in dynamic Guaymas Basin hydrothermal sediments. Nat. Commun. **9**: 4999. doi:10.1038/s41467-018-07418-0

Fagervold, S. K., P. E. Galand, M. Zbinden, F. Gaill, P. Lebaron, and C. Palacios. 2012. Sunken woods on the ocean floor provide diverse specialized habitats for microorganisms. FEMS Microbiol. Ecol. **82**: 616–628. doi:10.1111/j.1574-6941.2012.01432.x

Fry, B., and E. B. Sherr. editors. δ13C measurements as indicators of carbon flow in marine and freshwater ecosystems, Stable isotopes in ecological research; 1989. New York, NY: Springer New York.

Glassman, S. I., and J. B. H. Martiny. 2018. Broadscale ecological patterns are robust to use of exact sequence variants versus operational taxonomic units. mSphere **3**: e00148–e00118.

Goffredi, S. K., and V. J. Orphan. 2010. Bacterial community shifts in taxa and diversity in response to localized organic loading in the deep sea. Environ. Microbiol. **12**: 344–363. doi:10.1111/j.1462-2920.2009.02072.x

Hamdan, L. J., R. B. Coffin, M. Sikaroodi, J. Greinert, T. Treude, and P. M. Gillevet. 2013. Ocean currents shape the

microbiome of Arctic marine sediments. ISME J. **7**: 685–696. doi:10.1038/ismej.2012.143

Hamdan, L. J., J. J. Hampel, R. D. Moseley, R. L. Mugge, A. Ray, J. L. Salerno, and M. Damour. 2021. Deep-sea shipwrecks represent island-like ecosystems for marine microbiomes. Isme J. **15**: 2883–2891.

Hamdan, L. J., J. L. Salerno, A. Reed, S. B. Joye, and M. Damour. 2018. The impact of the deepwater horizon blowout on historic shipwreck-associated sediment microbiomes in the northern Gulf of Mexico. Sci. Rep. **8**: 1–14. doi:10.1038/s41598-018-27350-z

Harris, P. T. 2014. Shelf and deep-sea sedimentary environments and physical benthic disturbance regimes: A review and synthesis. Mar. Geol. **353**: 169–184. doi:10.1016/j.margeo.2014.03.023

Hoshino, T., H. Doi, G. Uramoto, L. Wörmer, R. R. Adhikari, and N. Xiao. 2020. Global diversity of microbial communities in marine sediment. Proc. Natl. Acad. USA **117**: 27587–27597. doi:10.1073/pnas.1919139117

Jørgensen, B. B., and A. Boetius. 2007. Feast and famine—Microbial life in the deep-sea bed. Nat. Rev. Microbiol. **5**: 770–781. doi:10.1038/nrmicro1745

Kalenitchenko, D., S. K. Fagervold, A. M. Pruski, G. Vétion, M. Yücel, N. Le Bris, and P. E. Galand. 2015. Temporal and spatial constraints on community assembly during microbial colonization of wood in seawater. ISME J. **9**: 2657–2670. doi:10.1038/ismej.2015.61

Kalenitchenko, D., M. Dupraz, N. Le Bris, C. Petetin, C. Rose, N. J. West, and P. E. Galand. 2016. Ecological succession leads to chemosynthesis in mats colonizing wood in sea water. ISME J. **10**: 2246–2258. doi:10.1038/ismej.2016.12

Kalenitchenko, D., E. Péru, L. C. Pereira, C. Petetin, P. E. Galand, and N. Le Bris. 2018. The early conversion of deep-sea wood falls into chemosynthetic hotspots revealed by in situ monitoring. Sci. Rep. **8**: 4–11. doi:10.1038/s41598-017-17463-2

Kallmeyer, J., R. Pockalny, R. R. Adhikari, D. C. Smith, and S. D'Hondt. 2012. Global distribution of microbial abundance and biomass in subseafloor sediment. Proc. Natl. Acad. Sci. USA **109**: 16213–16216. doi:10.1073/pnas.1203849109

Landy, E. T., J. I. Mitchell, S. Hotchkiss, and R. A. Eaton. 2008. Bacterial diversity associated with archaeological waterlogged wood: Ribosomal RNA clone libraries and denaturing gradient gel electrophoresis (DGGE). Int. Biodeterior. Biodegrad. **61**: 106–116. doi:10.1016/j.ibiod.2007.07.007

Lloyd, K. G., and others. 2013. Predominant archaea in marine sediments degrade detrital proteins. Nature **496**: 215–218. doi:10.1038/nature12033

Martin, B. D., D. Witten, and A. D. Willis. 2020. Modeling microbial abundances and dysbiosis with beta-binomial regression. The annals of applied statistics **14**: 94.

Mason, O. U., and others. 2014. Metagenomics reveals sediment microbial community response to deepwater horizon oil spill. ISME J. **8**: 1464–1475. doi:10.1038/ismej.2013.254

McMurdie, P. J., and S. Holmes. 2013. Phyloseq: An R package for reproducible interactive analysis and graphics of microbiome census data. PLoS One **8**: e61217. doi:10.1371/journal.pone.0061217

Middelburg, J. J., and J. Nieuwenhuize. 1998. Carbon and nitrogen stable isotopes in suspended matter and sediments from the Schelde Estuary. Mar. Chem. **60**: 217–225. doi:10.1016/S0304-4203(97)00104-7

Mugge, R. L., M. L. Brock, J. L. Salerno, M. Damour, R. A. Church, J. S. Lee, and L. J. Hamdan. 2019. Deep-sea biofilms, historic shipwreck preservation and the deepwater horizon spill. Front. Mar. Sci. **6**. doi:10.3389/fmars.2019.00048

Ogrinc, N., G. Fontolan, J. Faganeli, and S. Covelli. 2005. Carbon and nitrogen isotope compositions of organic matter in coastal marine sediments (the Gulf of Trieste, N Adriatic Sea): Indicators of sources and preservation. Mar. Chem. **95**: 163–181. doi:10.1016/j.marchem.2004.09.003

Orcutt, B. N., J. B. Sylvan, N. J. Knab, and K. J. Edwards. 2011. Microbial ecology of the Dark Ocean above, at, and below the seafloor. Microbiol. Mol. Biol. Rev. **75**: 361–422. doi:10.1128/mmbr.00039-10

Orsi, W. D. 2018. Ecology and evolution of seafloor and subseafloor microbial communities. Nat. Rev. Microbiol. **16**: 671–683. doi:10.1038/s41579-018-0046-8

Overholt, W. A., P. Schwing, K. M. Raz, D. Hastings, D. J. Hollander, and J. E. Kostka. 2019. The core seafloor microbiome in the Gulf of Mexico is remarkably consistent and shows evidence of recovery from disturbance caused by major oil spills. Environ. Microbiol. **21**: 4316–4329. doi:10.1111/1462-2920.14794

Podosokorskaya, O. A., E. A. Bonch-Osmolovskaya, A. A. Novikov, T. V. Kolganova, and I. V. Kublanov. 2013. Ornatilinea apprima gen. Nov., sp. nov., a cellulolytic representative of the class Anaerolineae. Int. J. Syst. Evol. Microbiol. **63**: 86–92. doi:10.1099/ijs.0.041012-0

Reeds, K. A., J. A. Smith, I. M. Suthers, and E. L. Johnston. 2018. An ecological halo surrounding a large offshore artificial reef: Sediments, infauna, and fish foraging. Mar. Environ. Res. **141**: 30–38. doi:10.1016/j.marenvres.2018.07.011

Ristova, P. P., C. Bienhold, F. Wenzhöfer, P. E. Rossel, and A. Boetius. 2017. Temporal and spatial variations of bacterial and faunal communities associated with deep-sea wood falls. PLoS One **12**: e0169906.

Ruff, S. E., and others. 2015. Global dispersion and local diversification of the methane seep microbiome. Proc. Natl. Acad. Sci. USA **112**: 4015–4020. doi:10.1073/pnas.1421865112

Salerno, J. L., B. Little, J. Lee, and L. J. Hamdan. 2018. Exposure to crude oil and chemical dispersant may impact marine microbial biofilm composition and steel corrosion. Front. Mar. Sci. **5**: 1–14. doi:10.3389/fmars.2018.00196

Seitz, K. W., C. S. Lazar, K. U. Hinrichs, A. P. Teske, and B. J. Baker. 2016. Genomic reconstruction of a novel, deeply

branched sediment archaeal phylum with pathways for acetogenesis and sulfur reduction. ISME J. **10**: 1696–1705. doi:10.1038/ismej.2015.233

Smith, C. R., A. G. Glover, T. Treude, N. D. Higgs, and D. J. Amon. 2015. Whale-fall ecosystems: Recent insights into ecology, paleoecology, and evolution. Ann. Rev. Mar. Sci. **7**: 571–596. doi:10.1146/annurev-marine-010213-135144

Stahl, D. A., and J. R. De La Torre. 2012. Physiology and diversity of ammonia-oxidizing archaea. Annu. Rev. Microbiol. **66**: 83–101. doi:10.1146/annurev-micro-092611-150128

Stieglitz, T. C. 2013. Habitat engineering by decadal-scale bioturbation around shipwrecks on the Great Barrier Reef midshelf. Mar. Ecol. Prog. Ser. **477**: 29–40. doi:10.3354/meps10167

Thompson, L. R., and others. 2017. A communal catalogue reveals Earth's multiscale microbial diversity. Nature **551**: 457–463. doi:10.1038/nature24621

Tolar, B. B., L. Reji, J. M. Smith, M. Blum, J. T. Pennington, F. P. Chavez, and C. A. Francis. 2020. Time series assessment of Thaumarchaeota ecotypes in Monterey Bay reveals the importance of water column position in predicting distribution–environment relationships. Limnol. Oceanogr. **65**: 2041–2055. doi:10.1002/lno.11436

Treude, T., and others. 2020. Biogeochemical consequences of nonvertical methane transport in sediment offshore northwestern Svalbard. J. Geophys. Res. Biogeosci. **125**: e2019JG005371. doi:10.1029/2019JG005371

Vuillemin, A., Z. Kerrigan, S. D'Hondt, and W. D. Orsi. 2020. Exploring the abundance, metabolic potential and gene expression of subseafloor Chloroflexi in million-year-old oxic and anoxic abyssal clay. FEMS Microbiol. Ecol. **96**: 1–14. doi:10.1093/femsec/fiaa223

Walker, S. J., T. A. Schlacher, and M. A. Schlacher-Hoenlinger. 2007. Spatial heterogeneity of epibenthos on artificial reefs: Fouling communities in the early stages of colonization on an East Australian shipwreck. Mar. Ecol. **28**: 435–445. doi:10.1111/j.1439-0485.2007.00193.x

Woodcroft, B. J., and others. 2018. Genome-centric view of carbon processing in thawing permafrost. Nature **560**: 49–54. doi:10.1038/s41586-018-0338-1

Yu, T., W. Wu, W. Liang, M. A. Lever, K. U. Hinrichs, and F. Wang. 2018. Growth of sedimentary Bathyarchaeota on lignin as an energy source. Proc. Natl. Acad. Sci. USA **115**: 6022–6027. doi:10.1073/pnas.1718854115

Zhao, R., J. M. Mogollón, S. S. Abby, C. Schleper, and J. F. Biddle. 2020*a*. Geochemical transition zone powering microbial growth in subsurface sediments. Proc. Natl. Acad. Sci. USA **117**: 32617–32626. doi:10.1073/pnas.2005917117

Zhao, R., Z. M. Summers, G. D. Christman, K. M. Yoshimura, and J. F. Biddle. 2020*b*. Metagenomic views of microbial dynamics influenced by hydrocarbon seepage in sediments of the Gulf of Mexico. Sci. Rep. **10**: 1–13. doi:10.1038/s41598-020-62840-z

Zhou, Z., G. X. Zhang, Y. Bin Xu, and J. D. Gu. 2018. Successive transitory distribution of Thaumarchaeota and partitioned distribution of Bathyarchaeota from the Pearl River estuary to the northern South China Sea. Appl. Microbiol. Biotechnol. **102**: 8035–8048. doi:10.1007/s00253-018-9147-6

Zinger, L., and others. 2011. Global patterns of bacterial beta-diversity in seafloor and seawater ecosystems. PLoS One **6**: 1–11. doi:10.1371/journal.pone.0024570

Zinke, L. A., C. Glombitza, J. T. Bird, H. Røy, B. B. Jørgensen, K. G. Lloyd, J. P. Amend, and B. K. Reese. 2019. Microbial organic matter degradation potential in Baltic Sea sediments is influenced by depositional conditions and in situ geochemistry. Appl. Environ. Microbiol. **85**: 1–18. doi:10.1128/AEM.02164-18

Zou, D., J. Pan, Z. Liu, C. Zhang, H. Liu, and M. Li. 2020. The distribution of Bathyarchaeota in surface sediments of the Pearl River Estuary along salinity gradient. Front. Microbiol. **11**: 1–13. doi:10.3389/fmicb.2020.00285

Acknowledgments

Funding for this study was provided by the National Oceanic and Atmospheric Administration's (NOAA) Ocean Exploration and Research Program under Cooperative Agreement NA18OAR0110286. We acknowledge the support of R/V *Point Sur's* Captain and Crew, Remotely Operated Vehicle *Odysseus* (Pelagic Research Services) team, and the members of the shipboard science party that contributed to this study. We thank Dr. Tina Treude (UCLA) and Dr. Kevin Dillon (USM) for help with geochemical analyses and MBL STAMPS 2019 workshop instructors and teaching assistants for providing valuable advice and tips regarding data analysis.

Conflict of Interest

None declared.

Submitted 15 April 2021
Revised 10 December 2021
Accepted 15 December 2021

Associate editor: Osvaldo Ulloa